Structure–Property Relationships of Anionic Exchange Membranes for Fe/Cr Redox Storage Batteries*

CHARLES ARNOLD, Jr., and ROGER A. ASSINK, *Sandia National Laboratories, Albuquerque, New Mexico 87185*

Synopsis

Membranes with lower area resistivity, higher selectivity, and reduced susceptibility toward fouling were required to improve the efficiency and lifetime of Fe/Cr redox storage batteries. The relationship of membrane structure to these electrochemical properties was not well understood. To gain a better understanding of structure–property relationships, a series of model membranes was synthesized in which the degree of crosslinking, ion exchange capacity, and porosity could be varied independently. This permitted the completion of several factorial studies in which the effect of each structural variable and interaction between variables could be defined and quantified. It was found that increasing the ion exchange capacity had a beneficial effect on all three electrochemical properties. Increasing the porosity reduced the resistivity and fouling but resulted in poorer selectivity. The degree of crosslinking had no effect on resistivity but improved selectivity and reduced fouling was observed when this parameter was increased. These relationships are consistent with theoretical models that have been proposed to account for the behavior of ion exchange membranes in general. From this data, empirical models were constructed which could be used to predict the area resistivity and water content of other anionic exchange membranes.

INTRODUCTION

Anionic exchange membranes are used in Fe/Cr redox storage batteries to separate the anolyte from the catholyte and provide electrical continuity.[1] Membranes with lower area resistivity, higher selectivity and reduced susceptibility toward fouling are required to improve the efficiency and lifetime of these batteries. In order to develop improved membranes, a better understanding of the relationships between these properties and such structural parameters as degree of crosslinking, ion exchange capacity, and porosity was needed. The primary objective of this work was to define the structure–property relationships of anionic membranes and determine if these relationships were consistent with theories that have been proposed to elucidate the behavior of ion exchange resins. A secondary goal was to develop empirical models which can be used to predict membrane performance. This kind of information should be useful for the development of improved membranes.

In this study we used factorially designed experiments to define the effect of the above structural variables for the following reasons: (1) the effect of a single structural variable at different levels of the other variables can be

*This work performed at Sandia National Laboratories was supported by the U.S. Department of Energy under Contract #DE-AC04-76DP00789.

Journal of Applied Polymer Science, Vol. 29, 2317–2330 (1984)

Published by John Wiley & Sons, Inc. CCC 0021-8995/84/072317-14$04.00

isolated; (2) interactions between variables can be identified; (3) both factor effects and interactions can be quantified and used to construct empirical models; and (4) reliable estimates of error can be obtained by pooling of the standard deviations. To carry out a factorial study such as this, it was necessary to prepare model membranes which were designed in such a way to allow all the structural variables to be varied independently.

EXPERIMENTAL

Experimental Design. This study involved three two level factorial experiments. Each experiment had a different range of independent variables. The range of the structural variables are given in Table I and depicted schematically in Figure 1. Nine membranes were fabricated for each experiment. These membranes represent eight (2^3) combinations of high and low levels for each of the structural variables and a midpoint. The midpoint membrane was included to increase the degrees of freedom and test for possible curvature in the trends. In the first matrix, the range of each structural variable was made sufficiently wide to insure that main effects could be distinguished from experimental error. Difficulties, however, were encountered in determining the selectivity of a few of these membranes because of their mechanical fragility. This problem was overcome by reducing the variable range. Reliable selectivity data were obtained in matrix 2. The variable range was contracted even further to obtain more data in what turned out to be the optimum region and to test empirical models developed using matrix 2. The methodology used to statistically analyze the data are given in Refs. 2–4.

Membrane Preparation. The model membranes were prepared via free radical polymerization of ethylene glycol dimethacrylate (EGDM), 4-vinylpyridine (4-VP), and 2-ethylhexylmethacrylate (2-EHM). All the monomers were obtained from Polysciences, Inc., and were distilled to remove inhibitors and possible contaminants. The membranes were rendered porous by carrying out the polymerization in the presence of isobutanol. Isobutanol increases the internal volume of the crosslinked network and is later removed by extraction with water. The membranes were reinforced with modacrylic cloth obtained from Uniroyal Co. (Style 7-002-163). The apparatus used to prepare the membranes is shown in Figure 2. In a typical preparation, the monomer mixture containing isobutanol and a small quantity ($\sim$ 0.5% by weight) of 2,2′-azobis-2,4-dimethylvaleronitrile (VAZO 52)

TABLE I
Range of Structural Variables

	Matrix no.					
	1		2		3	
Structural variable	Low	High	Low	High	Low	High
% Crosslinking	10	50	25	50	40	50
Ion exchange capacity (meq/dg)	0.9	4.1	2.2	4.1	3.3	4.1
% Porosity	20	40	20	40	20	30

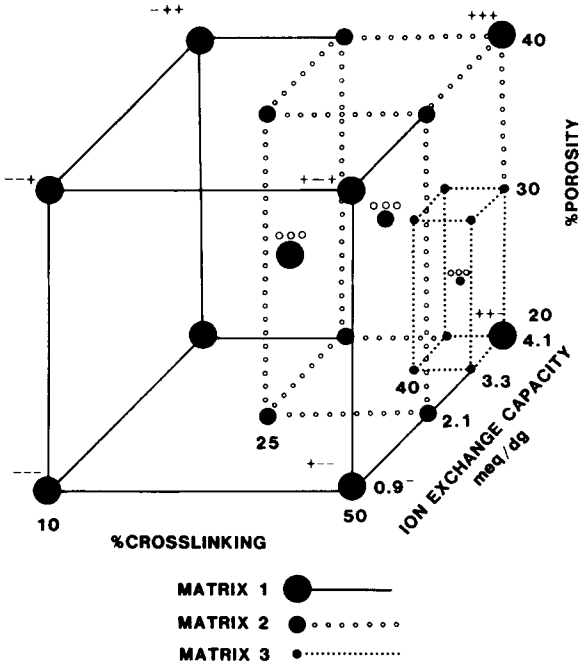

Fig. 1. Schematic plots of two-level factorial experiments.

was added to a 0.5 mm thick piece of modacrylic cloth contained between two glass plates. A 100-g weight was placed on top of the glass plates to avoid buoyancy effects and insure that the thickness of the membrane was uniform. The mixture was then cooled to 0°C degassed for 15 min at 45 Torr and placed in an oven which had been flushed out with nitrogen and heated to 45°C. After gelation of the membrane had occurred, the temperature was raised to 80°C and held there for 16 h. The membrane was then cooled, detached from the glass plates, and washed with methanol and water. The membranes were stored in deionized water prior to testing. The quantities of monomers and nonpolymerizing solvent used to formulate the model membranes are given in Table II. A photograph of a typical membrane is shown in Figure 3.

In order to carry out statistical analyses of the data, three samples of each membrane were prepared. The pooled standard deviations for matrices 1, 2, and 3 were 1.8, 0.83, and 0.78 $\Omega \cdot cm^2$, respectively. The higher deviation

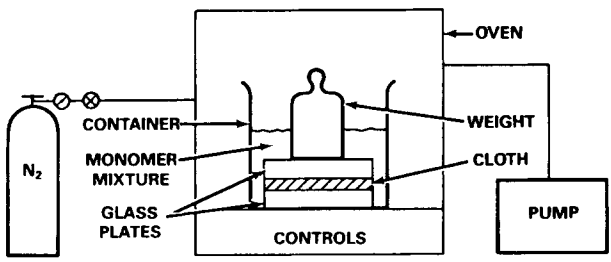

Fig. 2. Apparatus used to prepare membranes.

TABLE II
Quantities of Monomers and Nonpolymerizing Solvent (NMP) Used to Prepare Membranes

	Monomer											
	Ethylene glycol[a] dimethacrylate(g)			4-Vinylpyridine[b]			2-Ethylhexylmeth acrylate[c]			Isobutanol[d]		
Matrix no.:	1	2	3	1	2	3	1	2	3	1	2	3
Membrane code												
− − −	10	25	40	10	25	40	80	50	20	25	25	25
+ − −	50	50	50	10	25	40	40	25	10	25	25	25
− + −	10	25	40	50	50	50	40	25	10	25	25	25
+ + −	50	50	50	50	50	50	0	0	0	25	25	25
− − +	10	25	40	10	25	40	80	50	20	67	67	43
+ − +	50	50	50	10	25	40	40	25	10	67	67	43
− + +	10	25	40	50	50	50	40	25	10	67	67	43
+ + +	50	50	50	50	50	0	0	0	0	67	67	43
0 0 0	30	37.5	45	30	37.5	45	40	25	10	46	46	33

[a] EGDM.
[b] 4-VP.
[c] 2-EHM.
[d] Nonpolymerizing solvent

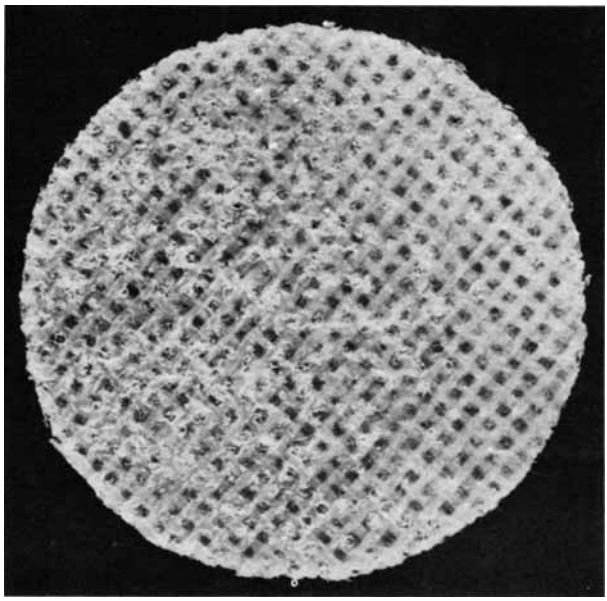

Fig. 3. Photograph of model membrane used in factorial studies.

obtained for matrix 1 was attributed to rather wide scatter with two of the membranes in which both the ion exchange capacity and the porosity were at their low levels, i.e., the $---$ and the $+ --$ membranes. With the exception of these two membranes, the spread in the area resistivity data was typically $\sim 15\%$. The pooled standard deviation of the iron permeation rates for matrices 2 and 3 were 78 and 27 μg Fe/cm^2 · h, respectively. Typically, data scatter was about $\pm 10\%$. The standard deviation for the fouling data was obtained using the midpoint membrane of matrix 2. Here the standard deviation was 124%, which represents an error of about 20%.

Membrane Evaluation. The two-piece Lucite fixture used to carry out the area resistivity measurements is shown in Figure 4. These measurements were conducted at 1 kHz in 1*N* HCl using platinum electrodes with

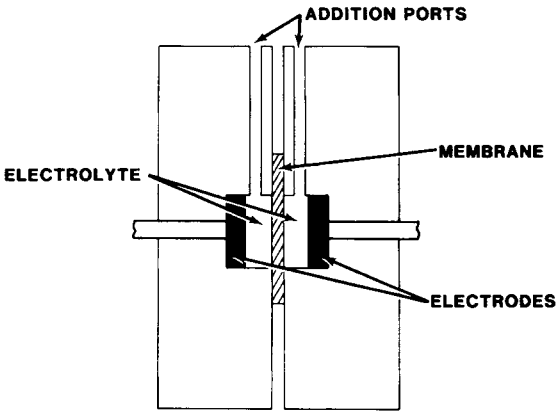

Fig. 4. Fixture used to measure area resistivity of membranes.

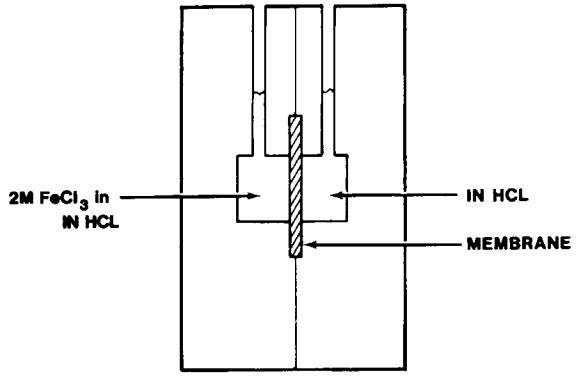

Fig. 5. Fixture used to determine iron transport rate through membranes.

a surface area of 2.84 cm^2 and a General Radio Corp. impedance bridge (Model 1650 A). In calculating the area resistivity of the membrane, corrections were made for the resistance of the electrolyte.

The two-part fixture used to determine the rate of iron transport through membranes is shown in Figure 5. The membrane to be tested was clamped in the center of the fixture. A solution of 2*M* FeCl, in 1*N* HCl, was then added to the right-hand cell. After 24 h, the concentration of iron in the right-hand cell was determined spectrophotometrically after reduction with hydroxylamine and complexation with 1,10-phenanthroline using a Cary Model 17 Spectrophotometer. This analytical procedure has been described in detail by Harvey et al.[5]

The extent of membrane fouling was determined by measuring the percent increase in area resistivity after exposure of the membrane to flowing solutions of 2*M* $FeCl_3$–1*N* HCl on one side and 1*N* HCl on the other for 24 h. No increase in area resistivity was found after 24 h under these conditions.

The water content of the membrane was determined from the weights of wet and dry samples of the membrane and the weight of the fabric backing.

$$\% \ H_2O \text{ content} = 100 \times \left(\frac{\text{wt wet sample} - \text{wt dry sample}}{\text{wt wet sample} - \text{backing wt}} \right)$$

Drying was accomplished by heating the membrane at 110°C for 1 h.

Structure of Model Membranes. The chemical structure of the model membranes is shown below. In this terpolymer, crosslinking is provided by the ethylene glycol dimethacrylate (EGDM) in the structure. Crosslinking is required

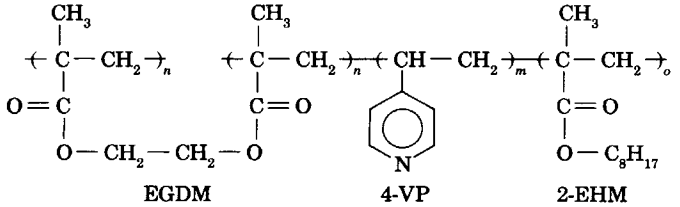

to insure that the membrane does not dissolve in the electrolyte. The 4-vinylpyridine (4-VP) units in the chain provide the ion exchange sites which, in turn, render the membrane selective. Selectivity can be defined as the ability of the membrane to block the transport of the positive electroactive ions, which, in this system, are the iron and chromium ions. The ion exchange sites also contribute to the conductivity of the membrane. 2-Ethylhexylmethacrylate is a diluant monomer which allows one to independently vary the relative concentrations of the other monomers and the nonpolymerizing solvent. The concentrations of ethylene glycol dimethacrylate, 4-vinylpyridine, and 2-ethylhexylmethacrylate are directly related to the degree of crosslinking, ion exchange capacity, and porosity of the membrane, respectively.[6,7]

RESULTS

The responses of the factorial matrix can be plotted in the form of a cube. The cube for the area resistivity of matrix 1 is shown in Figure 6. The numbers in the circles at each corner of the cube represent the response (in this case area resistivity), and the edges of the cube delineate the range of the structural variables. The main effect of each structural variable was obtained and quantified by subtracting the average of all the high level responses from the average of all the low level responses. High and low level responses correspond to parallel faces of the cube. Real effects were distinguished from error by comparing the response difference with the minimum significant factor effect. The latter was obtained from the pooled standard deviation of the entire matrix. The minimum significant factor effect was 1.6 $\Omega \cdot cm^2$ for matrix 1. Interactions between structural variables were obtained in a similar manner by subtracting the average responses of planes that run diagonally across the cube. By applying these operations to the cube shown in Figure 6 it can be shown that the main factor effects

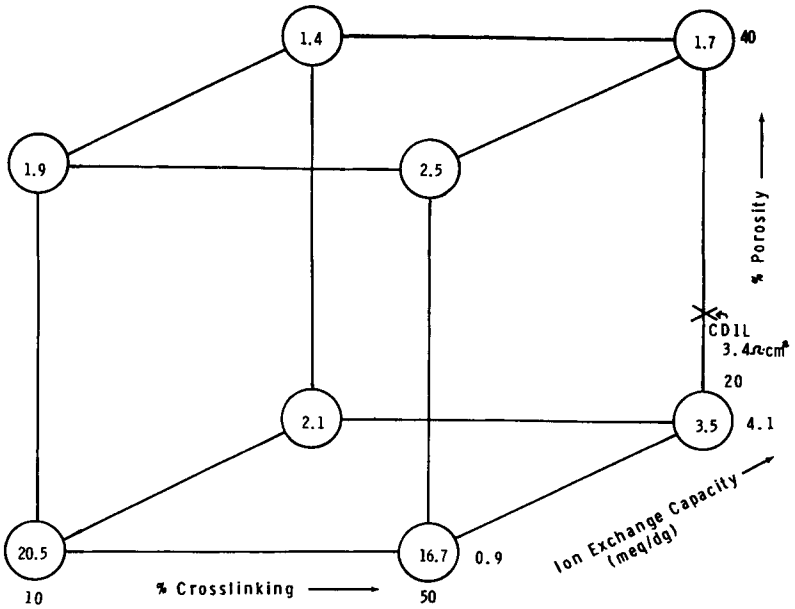

Fig. 6. Factorial plot of area resistivity (matrix 1).

on area resistivity existed for ion exchange capacity and porosity, but that the effect of crosslinking is negligible. Furthermore, there was a relatively strong negative interaction between ion exchange capacity and porosity, i.e., the effects are different at high and low levels of the other variables. Because the trends were linear, the following polynomial equation could be used to predict the resistivity of other membranes within the range of the matrix:

$$Y_R = 6.3 - 4.1(\text{IEC}) - 4.4(P) + 3.8(\text{IEC})(P) \quad (1)$$

where Y_R = predicted area resistivity, IEC = coded factor level of ion exchange capacity, and P = coded factor level for porosity. Terms that were not considered significant such as crosslinking were omitted.

When eq. (1) was used to predict the area resistivity of other model membranes within the range of the factorial experiment, fair agreement between the predicted responses and experimentally determined values was found. The predicted vs. observed responses are summarized in Table III.

The utility of this equation to approximate the area resistivity of membranes whose chemical structure was different from that of our model membranes was also demonstrated. The membrane used for this purpose was a developmental membrane (CD1L) obtained from Ionics Corp. This particular membrane was made from one mole of vinylbenzyl chloride and 2 mol of *N,N*-dimethylaminoethylmethacrylate.[8] The degree of crosslinking, ion exchange capacity, and porosity of this membrane were 50%, 4.0 meq/dg and 27.5%, respectively. Again, fair agreement between the predicted vs. experimental values for area resistivity was observed [calculated from eq. (1); 2.8 $\Omega \cdot \text{cm}^2$, experimental; 3.4 $\Omega \cdot \text{cm}^2$ in 1*N* HCl]. The location of this membrane on the factorial plot is shown in Figure 6.

The water contents of the model membranes were found to depend primarily on the porosity and ion exchange capacity of the membrane. There was a small effect attributable to crosslinking and an interaction was noted between crosslinking and ion exchange capacity. The trends were linear and could be modeled by the following equation:

$$Y_{H_2O} = 37 + 1.0(X_L) + 5.3(\text{IEC}) + 5.9(P) - 1.4(X_L)(\text{IEC}) \quad (2)$$

TABLE III
Area Resistivities Predicted from Eq. (1) vs. Experimental Area Resistivities

Membrane (matrix 3)	Predicted area resistivity ($\Omega \cdot \text{cm}^2$)	Observed area resistivity ($\Omega \cdot \text{cm}^2$)
1	6.43	5.00
2	6.43	5.11
3	2.80	2.96
4	2.80	3.5
5	4.09	3.83
6	4.09	3.63
7	2.20	2.15
8	2.20	2.76
9	3.88	3.26

where Y_{H_2O} = predicted water content (%), X_L = coded factor level of degree of crosslinking, IEC = coded factor level for ion exchange capacity, and P = coded factor level for ion porosity. Using eq. (2), it was found that a membrane with an ion exchange capacity of 3.34 meq/dg a crosslink density of 40% and a porosity of 30% would have a water content of 38.4%. This is the $--+$ membrane of matrix 3; its experimental water content was found to be 37.7%, a value that falls within the pooled standard deviation that was calculated for the whole matrix. Similar agreement was obtained when eq. (2) was applied to several other model membranes in matrix 3. In addition, it was found by linear regression analysis that there was some correlation between water content and area resistivity. The correlation coefficient was −0.88.

Factorial plots of the rate of permeation of iron through the membrane are shown in Figure 7. The effects of the structural variables can readily be extracted from this plot. It is apparent, for example, that increasing the porosity caused an increase in the rate of permeation. The effect of increasing the degree of crosslinking and the ion exchange capacity, however, were somewhat more complex. When the degree of crosslinking was increased at the low level of ion exchange capacity, the rate of permeation increased; we have no explanation for this somewhat puzzling result. The opposite effect was noted at the high level of ion exchange capacity. This indicates that the degree of crosslinking and ion exchange capacity interact strongly. While the overall effect of increasing the ion exchange capacity was to decrease the rate of permeation, this was not true in all regions of the matrix. For example, when the ion exchange capacity was increased from 2.1 to 4.1 meq/dg at the high level of crosslinking and low level of porosity, a minimum in the rate of permeation was observed at 3.3 meq/dg.

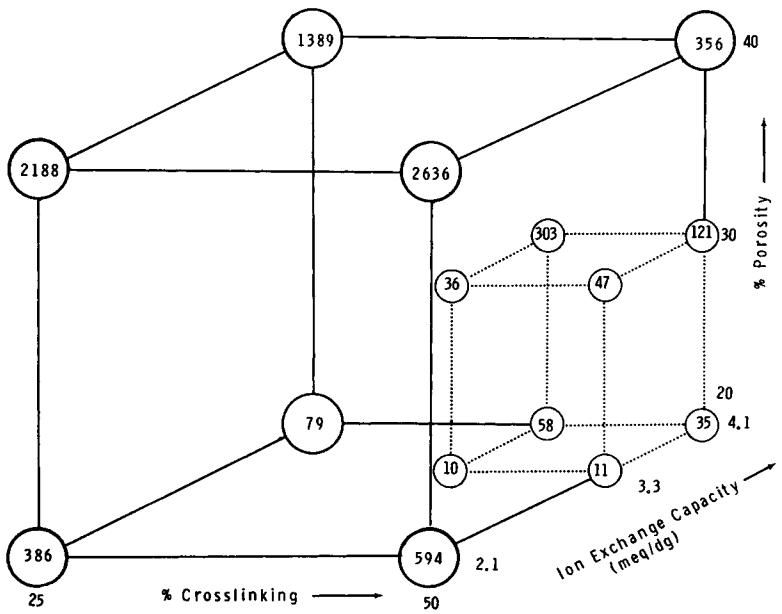

Fig. 7. Factorial plots of permeation (μg Fe/cm² · h): (○) matrix 2; (•) matrix 3.

Statistical analysis of the data, which included evaluation of permeation rates at the midpoints of both matrices, indicated that there was curvature in the trends. Consequently, we did not attempt to develop predictive models as we did for area resistivity and water content. Nevertheless, it is apparent from these experiments that optimum permeation rates can be found at high levels of crosslinking, low levels of porosity, and some intermediate level of ion exchange capacity. It is also evident from this data that iron permeation rates are quite sensitive to relatively small changes in the structural variables. Thus, changes of iron permeation rates of greater than 3 orders of magnitude were noted when the porosity was decreased from 40% to 20% and the ion exchange capacity was increased from 2.1 meq/dg to 3.3 meq/dg at a constant high (50%) level of crosslinking.

Factorial plots of fouling behavior are shown in Figure 8. Fouling decreased as the degree of crosslinking increased except at low levels of porosity and ion exchange capacity. This is evident from a comparison of the fouling data obtained at the two front corners of the cube. Statistical analysis of the data revealed that there were multiple interactions among all three of the structural variables. Furthermore, all of these effects deviated widely from linearity.

The structure–property relationships observed for all three factorial experiments are summarized in Table IV. This table indicates whether a membrane property, such as area resistivity, increases or decreases in response to an increase in each of the structural parameters. This is, in essence, the main effect of the structural variable. Also included in this table are all of the interactions that were observed and information concerning the linearity of the trends. It is clear from this table that increasing the ion exchange capacity had a beneficial effect on all three membrane

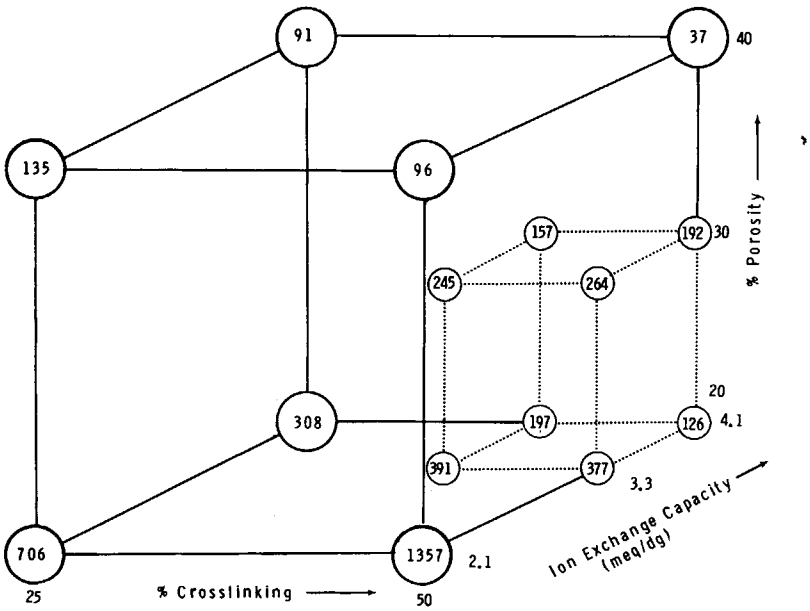

Fig. 8. Factorial plots of fouling behavior. (○) matrix 2; (•) matrix 3.

TABLE IV
Summary of Structure–Property Relationships Structural Variables (Increase)[a]

Property	IEC	P	XL	Interactions	Curvature
Area resistivity	Decrease	Decrease	No change	IEC/P	No
Permeation rate of Fe	Decrease	Increase	Decrease	IEC/P XL/P XL/IEC	Yes
Fouling	Decrease	Decrease	Decrease	IEC/P XL/P XL/IEC	Yes
H_2O content	Increase	Increase	No change	XL/IEC	No

[a] IEC = ion exchange capacity; P = nonpolymerizing solvent content (porosity); XL = degree of crosslinking.

properties and enhanced the water content of the membrane. Increasing membrane porosity reduced the area resistivity and fouling but had an adverse effect on selectivity. Thus, as one increases the porosity, there is a tradeoff to be made between area resistivity and fouling vs. selectivity. Water content also increased with increasing porosity. While the degree of crosslinking had no effect on area resistivity or water content, increasing the crosslink density had a beneficial effect on both selectivity and fouling. The structure–property relationships observed for selectivity and fouling are quite complex as evidenced by the existence of multiple interactions and nonlinearity in the trends.

DISCUSSION

The electrical conductivity of an ion exchange membrane immersed in an electrolyte is known to be a function of the concentration and mobility of the ionic species in the membrane.[9] It is also a function of the tortuosity of the membrane.[9] Tortuosity is defined as the effective path length of the migrating ions through the membrane which is made of a network of interlocking pores. Because these networks act as physical barriers to the migrating ions, ion mobility is effectively reduced. The effects of ion exchange capacity and porosity on the initial resistance of the membranes that were observed in our factorial experiments are consistent with this physical model. The concentration of the mobile counterions in the membrane should increase as the ion exchange capacity is increased. This, in turn, should result in an increase in electrical conductivity. This was, in fact, observed; i.e., the area resistivity of the membrane decreased with increasing ion exchange capacity. Furthermore, one would expect that the effective path length of the membrane would decrease with increased porosity and that this would also lead to increased electrical conductivity. Again, this was observed. According to the above physical model, the electrical conductivity is inversely proportional to the square of the tortuosity but only directly proportional to the concentration of the counterions.[9] Conceivably, this could account for the finding that a negative interaction existed between porosity and ion exchange capacity. Also noteworthy is the fact that the physical model contains no terms to account for the effect of

crosslinking in the membrane. In our factorial experiments it was shown that the effect of crosslinking on area resistivity was negligible.

According to the Donnan principle co-ions are partially excluded from ion exchange membranes.[10] This accounts for the separation of iron and chromium ions by the anionic membranes evaluated in this study. When an electrical potential is applied to these membranes, the negatively charged chloride ions (counterions) migrate through the membrane with relative ease and carry most of the current. In contrast, the positively charged iron and chromium ions, are repulsed by the fixed positive charges that line the pores of the membrane. Generally, the higher the concentration of these fixed positive charges, i.e., the higher the ion exchange capacity of the membrane, the greater is the exclusion effect.[11] It has also been reported that cation exclusion is favored by low porosity.[6] This seems reasonable. The larger the pore size, the less one would expect the repulsion effect to be. On these bases, therefore, one would predict that selectivity would increase with increasing ion exchange capacity and decreased porosity. These are precisely the effects that were observed in our factorial study.

It is well established that the degree of swelling decreases with increased crosslink density.[12] One would expect that more highly crosslinked membranes would be less permeable because of reduced internal volume of the network. This was, in fact, observed but only for membranes in which the ion exchange capacity was greater than 2.1 meq/dg.

It has been reported that the transport of iron through membranes from solutions of $FeCl_3$/HCl on one side to solutions of HCl on the other is considerably higher than the transport of chromium from similar solutions of $CrCl_3$/HCl and HCl.[7,8] This has been attributed to the fact that Fe^{+++} forms complexes with the chloride ion.[13] Thus, in strong HCl solutions of ferric chloride there exist the following complexes: $FeCl^{++}$, $FeCl_2^{+}$, $FeCl_4^{-}$, $FeCl_6^{-3}$. $FeCl_4^{-}$ and $FeCl_6^{-3}$ are negatively charged and should not be excluded from membranes which bear fixed positive charges. $FeCl^{++}$ and $FeCl_2^{+}$ would be partially excluded but to a lesser extent than Fe^{+++} because of their lower charge densities. Displacement of chloride associated with the fixed positive ions (the pyridinium ions) by the negative iron complexes is a distinct possibility. Given these complexities, it is not surprising that the rate of iron permeation varied so widely over the range of our factorial experiments and that interactions were found for all three structural variables.

Evidence has recently been found which indicates that the fouling of anionic membranes by strongly acidic solutions of ferric chloride is caused by loss of water from the membrane.[14] Most of this water loss can be accounted for by membrane shrinkage and displacement by the iron complexes. The beneficial effect of porosity and crosslinking on the rate of fouling of the model membranes is understandable in light of this fouling mechanism. For example, since the water content of high porosity membranes is higher than low porosity membranes, more water is available for ionic conduction after displacement and membrane shrinkage. More highly crosslinked membranes would be less prone to shrink and, consequently, foul less. Fouling rate also decreases with increasing ion exchange capacity.

Conceivably, membranes with high ion exchange capacity would be less prone to shrink. The presence of ionic groups in the backbone of polymers is known to enhance mechanical strength.[15] If some fraction of the fouling is caused by deactivation of the ion exchange sites, a membrane with more of these sites would be expected to foul to a lesser extent. The finding that there were interactions among all three structural variables and that the effects were not linear suggests that fouling is a relatively complex phenomenon.

The results of these factorial studies suggest that it should be possible to improve membrane performance in Fe/Cr redox batteries by increasing the ion exchange capacity and degree of crosslinking while adjusting the porosity to some intermediate level. One possible way of achieving this would be to incorporate ion exchange sites into the crosslinking element of membrane. Another possible synthetic route would be to crosslink a high ion exchange resin such as polyethyleneimine *in situ* using such agents as dihaloalkanes. These possibilities are being investigated.

SUMMARY AND CONCLUSIONS

The effect of the degree of crosslinking, ion exchange capacity, and porosity on the area resistivity, selectivity, and fouling characteristics of anionic exchange membranes was determined. This was accomplished by synthesizing and evaluating a series of model membranes in which the above-mentioned structural variables could be varied independently. This allowed the completion of several factorially designed experiments. It was found in this study that increasing the ion exchange capacity had a beneficial influence on all three electrochemical properties. Increasing the porosity resulted in reduced area resistivity and fouling but had an adverse effect on the selectivity of the membrane. Increasing the degree of crosslinking had no effect on area resistivity in the range of our experiments but did serve to enhance the selectivity and had a beneficial effect on fouling behavior.

For properties (area resistivity and water content) in which linear relationships were found with the structural parameters, it was possible to construct empirical models which could be used to predict the properties of other model membranes within the range of the factorial experiments. Furthermore, the model for area resistivity was a good predictor for membranes whose chemical constitution was markedly different than the model membranes. The complex structure–property relationships that were observed for selectivity and fouling precluded the construction of simple models for these properties. Nevertheless, the structure–property relationships found for the redox electrolytes were consistent with physical models that have been developed to elucidate the behavior of ion exchange membranes in general. The structure–property relationships that were identified in this study suggested that it should be possible to improve membrane performance by increasing the ion exchange capacity and degree of crosslinking while adjusting the porosity level to some value between the extremes of our experiments.

References

1. L. H. Thaller, "Recent Advances in Redox Flow Cell Storage Systems," DOE.NASA/1002-7914, NASA TM-79186, 1979.

2. W. G. Cochran and G. M. Cox, *Experimental Designs,* 2nd ed., Wiley, New York, 1957.

3. *Strategy of Experimentation,* rev. ed., DuPont, Wilmington, Del., October 1975.

4. C. R. Hicks, *Fundamental Concepts in the Design of Experiments,* Holt, Rinehart and Winston, New York, 1964.

5. A. E. Harvey, J. A. Smart, and E. S. Amis, *Anal. Chem.,* **27**(1), 26 (1955).

6. J. S. Ling and J. Charleston, *Proceedings of the Symposium on Ion Exchange, Transport and Interfacial Properties,* R. S. Yeo and R. P. Bruck, Eds., Electrochemical Society, Hollywood, FL, 1981, Vol. 81-2, p. 334.

7. S. S. Alexander, R. R. Geoffroy, and R. B. Hodgdon, "Anionic Selective Membranes," NASA CR-134931, 1975.

8. S. S. Alexander, R. B. Hodgdon, and W. A. Waite, "Anion Perselective Membranes," NASA CR-159599, 1979.

9. J. A. Lee, W. C. Maskell, and F. L. Tye, in *Membrane Separation Processes,* P. Meares, Ed. Elsevier, New York, 1976, p. 400.

10. F. Helfferich, *Ion Exchange,* McGraw-Hill, New York, 1962, p. 372.

11. Ref. 10, pp. 135–136.

12. P. J. Flory, *Principles of Polymer Chemistry,* Cornell University Press, Ithaca, N.Y., 1953, pp. 576–593.

13. N. V. Sidgwick, *The Chemical Elements and Their Compounds,* Oxford University Press, Oxford, 1950, Vol. II, p. 1366.

14. R. A. Assink, *Am. Chem. Soc., Polym. Prepr.,* Vol. 24, p.155, March (1983).

15. E. Besso and A. Eisenberg, *Proceedings of the Symposium on Ion Exchange, Transport and Interfacial Properties,* R. S. Yeo and R. P. Bruck, Eds., Electrical Society, 1981, Vol. 81-2, p. 197.

Received October 11, 1983
Accepted December 15, 1983